Received: 27 May 2022 | Accepted: 31 August 2022

DOI: 10.1111/1462-2920.16193

RESEARCH ARTICLE

Exopolysaccharides amylovoran and levan contribute to sliding motility in the fire blight pathogen *Erwinia amylovora*

Xiaochen Yuan | **Lauren I. Eldred** | **George W. Sundin**

Department of Plant, Soil, and Microbial Sciences, Michigan State University, East Lansing, Michigan, USA

Correspondence
George W. Sundin, Department of Plant, Soil, and Microbial Sciences, Michigan State University, East Lansing, Michigan 48824, USA.
Email: sundin@msu.edu

Funding information
National Institute for Food and Agriculture, Grant/Award Numbers: 2015-67013-23068, 2020-51181-32158; Michigan State University

Summary
Erwinia amylovora, the causative agent of fire blight, uses flagella-based motilities to translocate to host plant natural openings; however, little is known about how this bacterium migrates systemically in the apoplast. Here, we reveal a novel surface motility mechanism, defined as sliding, in *E. amylovora*. Deletion of flagella assembly genes did not affect this movement, whereas deletion of biosynthesis genes for the exopolysaccharides (EPSs) amylovoran and levan resulted in non-sliding phenotypes. Since EPS production generates osmotic pressure that potentially powers sliding, we validated this mechanism by demonstrating that water potential positively contributes to sliding. In addition, no sliding was observed when the water potential of the surface was lower than −0.5 MPa. Sliding is a passive motility mechanism. We further show that the force of gravity plays a critical role in directing *E. amylovora* sliding on unconfined surfaces but has a negligible effect when cells are sliding in confined microcapillaries, in which EPS-dependent osmotic pressure acts as the main force. Although amylovoran and levan are both required for sliding, we demonstrate that they exhibit different roles in bacterial communities. In summary, our study provides fundamental knowledge for a better understanding of mechanisms that drive bacterial sliding motility.

INTRODUCTION

Bacterial cells have evolved a range of active and passive motility mechanisms that enable migration under diverse environmental conditions including in liquids and on semisolid and solid surfaces (Henrichsen, 1972). Active motility mechanisms include swimming, swarming, twitching, and gliding motilities. Swimming occurs inside the medium, whereas the other forms of motility occur on the surface. In general, swimming and swarming are dependent on flagella, twitching is powered by type IV pili, and gliding motility is supported by several different types of motors depending on bacterial species (Harshey, 2003; Kearns, 2010; Mattick, 2002; McBride, 2001). Unlike active motility mechanisms, passive motility mechanisms such as sliding motility are not well characterized but have attracted attention in recent years (Henrichsen, 1972; Hölscher & Kovács, 2017; Kearns, 2010; Murray & Kazmierczak, 2008).

Exopolysaccharides (EPSs) are carbohydrate polymers secreted by bacteria that can be found either as capsules attached to the cell wall or as secreted slime in the surrounding environment (Leigh & Coplin, 1992; Sutherland, 1982; Whitfield et al., 2020). Mostly studied as the main components of the extracellular matrix of bacterial biofilms (Limoli et al., 2015; Sutherland, 2001), EPSs are also involved in the passive spreading of bacteria (Hölscher & Kovács, 2017; Nogales et al., 2012).

In *Bacillus subtilis*, Seminara et al. (2012) proposed a model in which osmotic pressure caused by the secretion of EPS drives sliding. EPS production causes an increase in osmotic pressure between the bacterial biofilm and the external environment, which promotes biofilm expansion likely through uptake of water from the external environment. Yan et al. (2017) reported a similar motility mechanism in *Vibrio cholerae*, the causal agent of pandemic disease cholera, but it is much less understood how pathogenic bacteria use EPS-mediated passive motility for infection. Besides EPS, other factors reported to affect sliding are surfactants (Hölscher & Kovács, 2017; Van Gestel et al., 2015), a *B. subtilis* hydrophobin protein BslA (Grau et al., 2015), the production of siderophore in *Sinorhizobium meliloti* (Grau et al., 2015; Nogales et al., 2012; Van Gestel et al., 2015), and glycopeptidolipids produced by *Mycobacterium smegmatis* (Recht & Kolter, 2001).

Erwinia amylovora is a Gram-negative enterobacterium that causes the disease fire blight in many economically important *Rosaceous* plants including apple, pear, blackberry, and raspberry (Griffith et al., 2003; Malnoy et al., 2012). Migration of this bacterium to the host plant flowers or leaves is thought to be facilitated by rain, wind, and insects (Holtappels et al., 2015; Puławska et al., 2017; Pusey, 2000; Thomson, 1986). On flowers, *E. amylovora* populations develop on stigmas, following which a flagella-dependent motility mechanism and free moisture are needed to facilitate the movement of bacterial cells into flowers. *E. amylovora* enters into the flower via natural openings in flower nectaries (Bayot & Ries, 1986). Infection of flowers, leaves at shoot tips, and stems of the apple host by *E. amylovora* is mediated by the type III secretion system (T3SS) (Malnoy et al., 2012). Infection occurs in cortical parenchyma cells layers of the host, and *E. amylovora* cells are present in the intercellular region or apoplast (Kharadi et al., 2021). Flagella are not required for cell spreading in the apoplast, and several studies have demonstrated that *E. amylovora* loses flagella once inside the plant and flagella-deficient strains exhibit similar spreading rates in young apple leaves compared to the wild type (Bayot & Ries, 1986; Cesbron et al., 2006; Holtappels et al., 2018; Raymundo & Ries, 1981). Systemic downward spreading of *E. amylovora* in trees via the apoplast is rapid, but the underlying mechanism remains largely elusive. For example, *E. amylovora* cells were detected in tissues >50 cm below the inoculated shoot tips of apples 11 days after inoculation and in the susceptible rootstock 3 weeks after inoculation (Momol et al., 1998).

Erwinia amylovora forms biofilms *in planta*, a process that relies on the production of three EPSs, amylovorna, levan, and cellulose (Castiblanco & Sundin, 2016; Kharadi et al., 2021; Malnoy et al., 2012). Amylovoran is a high-molecular-weight acidic heteropolysaccharide, consisting of a pentasaccharide repeating subunit containing galactose and glucuronic acid in a ratio of 4:1 (Nimtz et al., 1996). Levan is a simple homopolymer of fructose synthesized extracellularly from sucrose by levansucrase (Seemüller & Beer, 1977) and cellulose is a homopolymer of glucose residues (Ross et al., 1991). *E. amylovora* mutants deficient in amylovoran production are nonpathogenic, and levan and cellulose production mutants are reduced in virulence (Bellemann & Geider, 1992; Castiblanco & Sundin, 2018; Geier & Geider, 1993; Koczan et al., 2009), illustrating the importance of these EPSs to *E. amylovora* pathogenesis. We are interested in motility mechanisms driving the systemic movement of *E. amylovora* through the apple host, and we hypothesized that sliding motility represented an important mechanism for host invasion. In the present work, we studied how *E. amylovora* cells migrate on surfaces without the presence of flagella. We characterized an EPS-mediated sliding motility mechanism and identified two EPSs, amylovoran and levan, required for this movement. Water is important for plant–microbe interactions (Aung et al., 2018; Beattie, 2011). We provided further evidence showing that water potential positively regulates sliding, suggesting that osmotic-driven water flow is the main force for *E. amylovora* sliding motility.

EXPERIMENTAL PROCEDURES

Bacterial strains, plasmids, primers, and media

The bacterial strains and plasmids used in this study are listed in Table 1. *E. amylovora* and *P. syringae* strains were grown in LB medium at 28°C. *Escherichia coli* strains were grown in LB broth medium at 37°C. Swimming and swarming assays were conducted in MM medium (Na_2HPO_4 at 6 g/L, KH_2PO_4 at 3 g/L, NaCl at 0.5 g/L, NH_4Cl at 1 g/L, $MgSO_4{\cdot}7H_2O$ at 0.2 g/L, $CaCl_2$ at 0.1 g/L, nicotinic acid at 0.2 g/L, thiamine hydrochloride at 0.2 g/L, and sucrose at 20 g/L; Falkenstein et al., 1989) solidified with 0.2% w/v or 0.4% of agar. The sliding motility of *E. amylovora* was determined on surfaces of 1.0, 1.5, or 2.0 w/v % agar MM, MM-sorbitol (modified MM containing 20 g/L of sorbitol instead of sucrose), or MM supplemented with various concentrations of NaCl. Amylovoran production assays were conducted in modified basal medium A (MBMA) (KH_2PO_4 at 3 g/L, K_2HPO_4 at 7 g/L, $(NH_4)_2SO_4$ at 1 g/L, citric acid at 0.5 g/L, $MgSO_4$ at 0.03 g/L; Edmunds et al., 2013) containing 1% w/v sorbitol. Antibiotics were added as needed to media at the following concentrations: ampicillin (Ap; 100 μg/ml), chloramphenicol (Cm; 10 μg/ml), gentamicin (Gm; 15 μg/ml), or kanamycin (Km; 30 μg/ml). Genome

TABLE 1 Strains and plasmids used in this study

Strains and plasmids	Relevant characteristics	References or source
Erwinia amylovora		
Ea110	Wild type	Ritchie and Klos (1977)
Ea1189	Wild type	Zhao, Sundin, and Wang (2009)
Δ*flhDC1*	Δ*flhDC1*::*Km*; Km^r, EAM_2034 and EAM_2033 deletion mutant in Ea1189	This study
Δ*motA1*	Δ*motA1*::*Km*; Km^r, EAM_2032 deletion mutant in Ea1189	This study
Δ*fliC*	Δ*fliC*::*Cm*; Cm^r, EAM_2067 deletion mutant in Ea1189	This study
Δ*ams*	Δ*ams*, clean mutant, deletion of 12-gene *ams* operon in Ea1189	Zhao, Sundin, and Wang (2009)
Δ*lsc*	Δ*lsc*::*Cm*; Cm^r, EAM_3468 deletion mutant in Ea1189	This study
Δ*bcsA*	Δ*bcsA*, clean mutant, EAM_3387 deletion mutant in Ea1189	Castiblanco and Sundin (2018)
Δ*ams*Δ*lsc*	Δ*ams*Δ*lsc*::*Km*; Km^r, deletion mutant of 12-gene *ams* operon and EAM_3468 in Ea1189	This study
Δ*amsG*	Δ*amsG*::*Km*; Km^r, EAM_2174 deletion mutant in Ea1189	This study
Δ*flhDC1*Δ*ams*	Δ*ams*Δ*flhDC1*::*Km*; Km^r, deletion mutant of 12-gene *ams* operon, EAM_2034, and EAM_2033 in Ea1189	This study
Δ*flhDC1*Δ*lsc*	Δ*lsc*::*Cm*Δ*flhDC1*::*Km*; Km^r and Cm^r, EAM_3468, EAM_2034, and EAM_2033 deletion mutant in Ea1189	This study
Δ*flhDC1*Δ*bcsA*	Δ*bcsA*Δ*flhDC1*::*Km*; Km^r, EAM_3387, EAM_2034, and EAM_2033 deletion mutant in Ea1189	This study
Δ*edcC*	Δ*edcC*, clean mutant, EAM_1504 deletion mutant in Ea1189	Edmunds et al. (2013)
Δ*edcE*	Δ*edcE*, clean mutant, EAM_2435 deletion mutant in Ea1189	Edmunds et al. (2013)
Δ*edcC*Δ*edcE*	Δ*edcC*Δ*edcE*, clean mutant, EAM_1504 and EAM_2435 deletion mutant in Ea1189	Edmunds et al. (2013)
Δ*amyR*	Δ*amyR*::*Cm*; Cm^r, EAM_1300 deletion mutant in Ea1189	This study
Escherichia coli		
DH5α	*supE*44 Δ*lac*U169 (*ϕ*80*lacZ*ΔM15) *hsdR*17 *recA*1 *endA*1 *gyrA*96 *thi*-1 *relA*1	Lab stock
Pseudomonas syringae		
DC3000	Wild type	Lab stock
Plasmids		
pKD4	Template plasmid for kanamycin cassette, Km^r	Datsenko and Wanner (2000)
pKD3	Template plasmid for chloramphenicol cassette, Cm^r	Datsenko and Wanner (2000)
pKD46	Arabinose-inducible lambda red recombinase, Ap^r	Datsenko and Wanner (2000)
pBBR1-MCS5	Broad-host-range plasmid, Gm^r	Kovach et al. (1995)
pMP2444	*gfp* expressed from *lac* promoter, pBBR1-MCS5, Gm^r	Stuurman et al. (2000)
pBBR1-P$_{nptII}$-*mCherry*	*mCherry* expressed from *nptII* promoter, pBBR1-MCS5, Gm^r	This study
pBBR1-*amyR*	*amyR* cloned in pBBR1-MCS5, Gm^r	This study
pBBR1-*amsG*	*amsG* cloned in pBBR1-MCS5, Gm^r	This study
pBBR1-*lsc*	*lsc* cloned in pBBR1-MCS5, Gm^r	This study
pBBR1-*edcC*	*edcC* cloned in pBBR1-MCS5, Gm^r	This study
pBBR1-*edcE*	*edcE* cloned in pBBR1-MCS5, Gm^r	This study
pmCherry_NAT	Template plasmid for *mcherry*, Km^r	Roth and Chilvers (2019)
pPNptGreen	*gfp* expressed from *nptII* promoter, pPROBE-KT, Km^r	Axtell and Beattie (2002)
pPProGreen	*gfp* expressed from *proU* promoter, pPROBE-KT, Km^r	Axtell and Beattie (2002)

Abbreviations: Ap^r, ampicillin resistance; Cm^r, chloramphenicol resistance; Gm^r, gentamicin resistance; Km^r, kanamycin resistance.

(CP055227) and plasmid (CP055228) sequences of *E. amylovora* strain Ea1189 were retrieved from the National Center for Biotechnology Information (Yu et al., 2020). Oligonucleotide primers used for cloning are listed in Table S1.

Construction of mutant and complementation

Deletion mutants of *flhDC1*, *motA1*, *fliC*, *amsG*, *amyR*, and *lsc* were constructed using the red recombinase method (Datsenko & Wanner, 2000), and the method was recently described elsewhere (Yuan et al., 2022). Complementation strains were constructed by cloning the putative promoter and open reading frame (ORF) regions of target genes into the plasmid pBBR1-MCS5 (Table 1), followed by electroporation of the resulting plasmids into *E. amylovora*.

Swimming and swarming motility assays

Swimming and swarming motility assays were performed in MM containing 0.2% or 0.4% of agar. In brief, bacterial cells grown in LB were incubated at 28°C until the optical density at 600 nm (OD_{600}) reached ~1.0, corresponding to the mid- to late-exponential growth phase. Values of OD_{600} were measured using a Tecan Spark plate reader (Tecan, Männedorf, Switzerland). A total of 5 μl (approximately 2.5×10^7 cells) of bacterial cultures were spotted in the centre of MM plates, and the inoculated plates were incubated at 28°C for 48 h and photographed. Diameters of the radial area representing the motility of swimming and swarming were measured and quantified using ImageJ (Abràmoff et al., 2004).

Apple shoot virulence, levansucrase activity, and amylovoran production assays

Apple shoot virulence and levansucrase activity assays were performed as recently described (Yuan et al., 2022). Amylovoran production was determined in supernatants of bacterial cultures using a turbidity assay with cetylpyrimidinium chloride (CPC) (Bellemann et al., 1994). Briefly, cells grown in MBMA medium supplemented with 1% sorbitol were incubated at 28°C with shaking (220 rpm) for 48 h. The 200 μl of the supernatant were then mixed with 20 μl of CPC (50 mg/ml) for 10 min, and amylovoran production was calculated by measuring the resulting turbidity of mixtures at OD_{600} and normalized to the OD_{600} values of the culture.

Sliding motility, biomass, and bacterial population assays

The sliding motility of *E. amylovora* was assessed on surfaces of MM plates containing various concentrations of agar. A total of 5 μl of overnight bacterial cultures in LB ($OD_{600} = 1.0$) was spotted on MM plates. The inoculated plates were then incubated at 28°C on a flat surface and imaged daily. Sliding areas were quantified from photographs of inoculated plates using ImageJ. For bacterial sliding on inclined or declined surfaces, cells were first inoculated on one side of square MM plates and incubated at 28°C for 48 h on a flat surface. Plates were then placed on tilted surfaces, incubated for 16 h, and the length of sliding was measured. Inclined (+) or declined (−) angles were measured using a protractor and adjusted based on the horizontal line.

To create confined microcapillaries, warm 1.5% agar MM were filled into 2 ml microcentrifuge tubes, each containing a 22 G × 3.8 cm hypodermic needle (BD, Franklin Lakes, NJ, U.S.A.), and solidified at room temperature for 2 h. Needles were then removed, and tubes were baked with the cap open at 28°C for 12 h to evaporate condensed water in the microcapillary. For sliding motility, bacterial cells were transferred from LB plates to the open end of the microcapillary using a pipette tip.

For measuring biomass and bacterial population size of *E. amylovora* during sliding, bacterial biomass produced on 1.5% agar plates was harvested with a loop and suspended in a pre-weighed 0.5× PBS buffer. The weight gain was determined which represents the amount of biomass produced by *E. amylovora*. Bacterial cells were resuspended in 0.5× PBS buffer following which the cell number was determined by serial dilution and plate counting. To simultaneously quantify bacterial populations around the inoculated spot and the sliding area, bacterial biomass around the inoculated spot was collected using a 6 mm standard biopsy punch, and the remaining biomass around the sliding area was collected with a loop.

GFP transcriptional activity assay

To measure the transcriptional activities of P_{proU}-*gfp* and P_{nptII}-*gfp*, *E. amylovora* cells carrying reporter plasmids pPProGreen or pPNptGreen slid on 1.5% agar MM containing various concentrations of NaCl were harvested, respectively. Cells were resuspended and washed with 0.5× PBS buffer. The GFP intensity and OD_{600} values were measured using the Tecan Spark plate reader (Tecan, Männedorf, Switzerland) with excitement at 488 nm and emission detection at 435 nm. The reported GFP fluorescence was normalized to the OD_{600} value of bacterial suspensions.

Biosurfactant detection and cell surface hydrophobicity assays

Biosurfactant detection assay was performed using an atomized oil assay as previously described, with a few modifications (Burch et al., 2010). Bacteria grown overnight were spotted onto LB or MM agar plates and incubated at 28°C for 48 h. A fine stream of light paraffin oil (ThermoFisher Scientific, Waltham, MA, USA) was applied onto the plate using an airbrush with an air pressure of 1055 g/cm^2 (master airbrush model G22; TCP Global Co., San Diego, CA, USA). Halos of the biosurfactant were visualized and imaged immediately after spray. Oil droplets were observed using the Leica Zoom 2000 stereomicroscope (Leica microsystems, Wetzlar, Germany).

Cell surface hydrophobicity was measured using the hexadecane partitioning method (van Loosdrecht et al., 1987). Bacterial cells from overnight LB cultures were harvested and washed three times with 0.5× PBS buffer. Cells were then resuspended in 1 ml 0.5× PBS buffer and the OD_{540} values were determined. The 250 μl of *n*-hexadecane (Sigma-Aldrich, St. Louis, MO, USA) was then added to each cell suspension, and the suspensions were vortexed for 10 min. The resulting mixtures were incubated at 37°C for 30 min. The OD_{540} of the aqueous layer was measured against a blank of hexadecane-extracted PBS. Cell surface hydrophobicity was calculated as follows: cell surface hydrophobicity (in %) = 100× (final OD/initial OD).

Construction of the pBBR1-P_{nptII}-*mCherry* plasmid and confocal microscopy analysis

The *nptII* promoter was amplified from the plasmid pKD4 with primers *nptII*-F and *nptII*::*mCherry*-Rc (Table S1), resulting in a 279-bp DNA fragment. The 709-bp *mCherry* fragment was amplified from the plasmid pmCherry_NAT with a set of primers, *nptII*::*mCherry*-F and *mCherry*-Rc (Table S1). As the primer *nptII*::*mCherry*-Rc was designed to include the reverse complement sequence of *nptII*::*mCherry*-F, a crossover PCR was performed using the above PCR products as templates with primers *nptII*-F and *mCherry*-Rc to generate the *nptII*::*mCherry* fragment, followed by purification, digestion with XbaI and HindIII restriction enzymes, and ligation with the plasmid pBBR1-MCS5 digested by the same enzymes. The resulting plasmid was confirmed by sequencing and transformed into *E. amylovora* strain Ea1189 or various EPS-deficient mutants by electroporation.

E. amylovora cells expressing *gfp* from the plasmid pMP2444 or *mCherry* from the plasmid pBBR1-P_{nptII}-*mCherry* were observed for their sliding behaviour using confocal microscopy. Settings for the Nikon A1-Rsi confocal laser scanning microscope (Nikon Instruments, Inc., Tokyo, Japan) were recently described (Zhong et al., 2021). For image acquisition of the entire bacterial sliding area, multiple images were automatically collected across the bacterial film, with a 15% overlap between each image, and stitched together to form one large-area image using the Nikon NIS-Elements AR software. Briefly, for each field of view within the large-area scan, confocal images were collected in 20 μm increments through an average thickness of 100 μm. For each confocal series, a maximum intensity projection (MIP) image was generated, representing the brightest intensity pixels through the Z-depth. MIP images across the bacterial film were then stitched together to form a single large-area MIP image.

Statistical analysis

Means and standard deviations of experimental results were calculated using Excel, and mean comparisons were performed using a two-tailed student's *t*-test (Microsoft, Redmond, WA) or Fisher's least significant difference test using R software (https://www.R-project.org).

RESULTS

Flagella are required for in vitro swimming and swarming but not for apoplastic spreading of *E. amylovora*

Bacteria rotate flagella to swim in planktonic environments or swarm over surfaces (Berg, 2003; Kearns, 2010; Minamino et al., 2008). We confirmed the function of flagella in *E. amylovora* by comparing the swimming and swarming behaviours of the wild-type (WT) *E. amylovora* strain Ea1189 with those of three independent flagellar-deficient mutants, Ea1189Δ*flhDC1* (flagellar master regulator encoding genes) (Wang et al., 2006), Ea1189Δ*motA1* (flagellar motor complex encoding gene) (Blair & Berg, 1990), and Ea1189Δ*fliC* (flagellin encoding gene) (Fitzgerald et al., 2014). We found that cells of Ea1189 swam or swarmed symmetrically from the inoculated spots with diameters of ~4.0 cm in minimal medium (MM) solidified with 0.2% of agar and of ~2.5 cm in 0.4% agar MM at 2 days post-inoculation (dpi), respectively (Figure 1A,B). In contrast, flagella-deficient mutants were non-motile in both media (Figure 1A,B), which appeared consistent with the results from other studies (Schachterle et al., 2019; Zhao et al., 2011; Zhao, Wang, et al., 2009).

We also compared the disease progression between Ea1189 and flagella-deficient mutants when cells were inoculated at the tip of apple shoots through

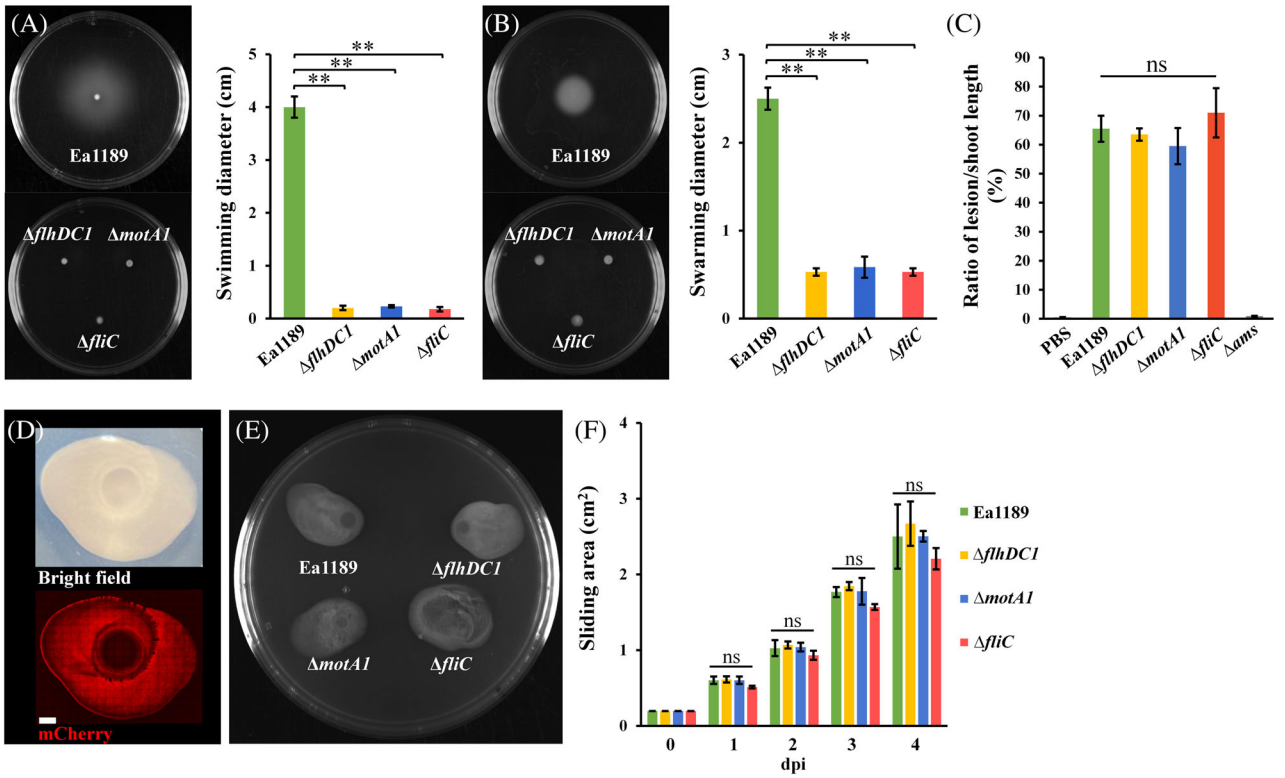

FIGURE 1 Flagella are required for swimming and swarming but not for sliding or apoplastic spreading in *E. amylovora*. (A) Swimming and (B) swarming motilities were determined in wild-type (WT) *E. amylovora* strain Ea1189 and flagella-deficient mutants, Ea1189Δ*flhDC1*, Ea1189Δ*motA1*, and Ea1189Δ*fliC*, in 0.2% and 0.4% agar minimal medium (MM), respectively. Images were taken 2 days post inoculation (dpi). Mean and standard deviation ($n = 3$) are shown. (C) Apple shoots inoculation assay was performed using the above-mentioned strains by a scissor-dip method described in Experimental Procedures section. At 10 dpi, the percentage of lesion/shoot length for bacterial spreading in the apoplast was calculated. Mean and standard deviation ($n = 5$) are shown. (D) the surface sliding of Ea1189 harbouring the plasmid pBBR1-P_{nptII}-*mCherry* was determined on 1.5% agar MM. Microphotographs were captured using light microscopy with incident lighting (upper graph) and confocal microscopy detecting mCherry fluorescence (lower graph), respectively, at 4 dpi. The scale bar represents 0.2 cm. Sliding motilities (E) and overall sliding areas (F) were compared between WT Ea1189 and Ea1189 flagella-deficient mutants on 1.5% agar MM at 0, 1, 2, 3, and 4 dpi. The image was captured at 3 dpi. Mean and standard deviation ($n = 3$) are shown. One representative experiment was chosen, and three (two for the apple shoots assay) independent experiments were conducted. Asterisks indicate statistically significant differences of the means (ns = not significant, $p > 0.05$; $^{**}p < 0.01$ by Student's *t*-test).

wounding. At 10 dpi, necrosis was observed in Ea1189-inoculated shoots with a percentage of lesion/shoot length of approximately 65%. Meanwhile, shoots inoculated with flagella-deficient mutants exhibited similar lesion lengths to those inoculated with Ea1189, whereas no visible lesions were observed in shoots inoculated with the amylovoran deficient mutant Ea1189Δ*ams* (Figure 1C). Deletion of *ams* did not affect swimming or swarming in vitro (data not shown). Taken together, our data strongly suggest that flagella and flagella-dependent motility mechanisms are not required for the migration of *E. amylovora* in the apoplast.

E. amylovora exhibits surface motility independent of flagella

To explore the motility mechanisms independent of flagella, we examined the movement of *E. amylovora* on MM solidified with 1.5% agar, generating a relatively dry and solid surface. Notably, cells of Ea1189 formed slimy colonies at the inoculated spot and gradually expanded outward in an asymmetric manner (Figure S1). This movement pattern differed from those of the symmetrical movements observed for swimming or swarming in vitro (Figure 1A,B) and was further validated by visualizing cells constitutively expressing the red fluorescent protein-encoding gene *mCherry* from the plasmid pBBR1-MCS5 (Figure 1D). In addition, our data confirmed that flagella are not required for this surface movement, as three flagella-deficient mutants (Ea1189Δ*flhDC1*, Ea1189Δ*motA1*, and Ea1189Δ*fliC*) exhibited motility areas that were not significantly different from WT Ea1189 over a 4-day growth period (Figure 1E,F). Taken together, our data support a model that a previously uncharacterized motility mechanism enables surface migration of *E. amylovora* in a flagella-independent manner. We named this sliding motility as it is consistent with the description of the

passive biofilm expansion and sliding motility from studies of several other bacterial species such as *B. subtilis* and *V. cholerae* (Henrichsen, 1972; Hölscher & Kovács, 2017; Seminara et al., 2012; Yan et al., 2017). Interestingly, we found that unlike *B. subtilis* slides on rich media such as lysogeny broth (LB) by a flagella-independent mechanism (Fall et al., 2006), *E. amylovora* did not slide on LB medium (data not shown), suggesting that sliding motility might be species-specific in bacteria.

Two EPSs, amylovoran and levan, are required for the sliding motility of *E. amylovora*

E. amylovora produces three EPSs, amylovoran, levan, and cellulose (Castiblanco & Sundin, 2018; Malnoy et al., 2012), which led to a question that whether the above-described sliding motility is associated with the secretion of EPSs. For this purpose, we tested sliding phenotypes of mutant bacteria defective in the biosynthesis of individual EPSs and compared them with that of the WT Ea1189. Deletion of the *ams* operon, encoding 12 amylovoran biosynthetic enzymes (Bugert & Geider, 1995), the first *ams* gene *amsG*, or the levansucrase encoding gene *lsc* (Seemüller & Beer, 1977) resulted in cells that were unable to slide on 1.5% agar MM (Figures 2A,B and S2). Deletion of both *ams* and *lsc* (Ea1189Δ*ams*Δ*lsc*) significantly hindered sliding motility to a level the same as the single deletion mutants (Figure 2A,B). In contrast, deletion of the cellulose biosynthesis gene *bcsA* (Castiblanco & Sundin, 2018) had a negligible impact on sliding motility (Figure 2A,B). To further ensure that sliding motility is driven by the production of EPSs, *in trans* expression of amylovoran or levan biosynthesis genes was conducted in EPS-deficient mutants and found WT levels of the sliding phenotype (Figure S2). Since we did not observe strong correlations between the production of these two EPSs (Figure S3) and Geier and Geider (1993) previously found normal amounts of amylovoran in several transposon mutants of *lsc*, these data indicate that both amylovoran and levan play a key role for sliding.

Next, we speculated that the absence of flagella would not affect EPS-mediated sliding motility. Indeed, no changes were found between the sliding motility of Ea1189Δ*flhDC1* and that of the double mutant Ea1189Δ*flhDC1*Δ*bcsA* (Figure S4), confirming that cellulose is not involved in sliding. In contrast, double mutants of Ea1189Δ*flhDC1*Δ*ams* and Ea1189Δ*flhDC1*Δ*lsc* were non-motile (Figure S4).

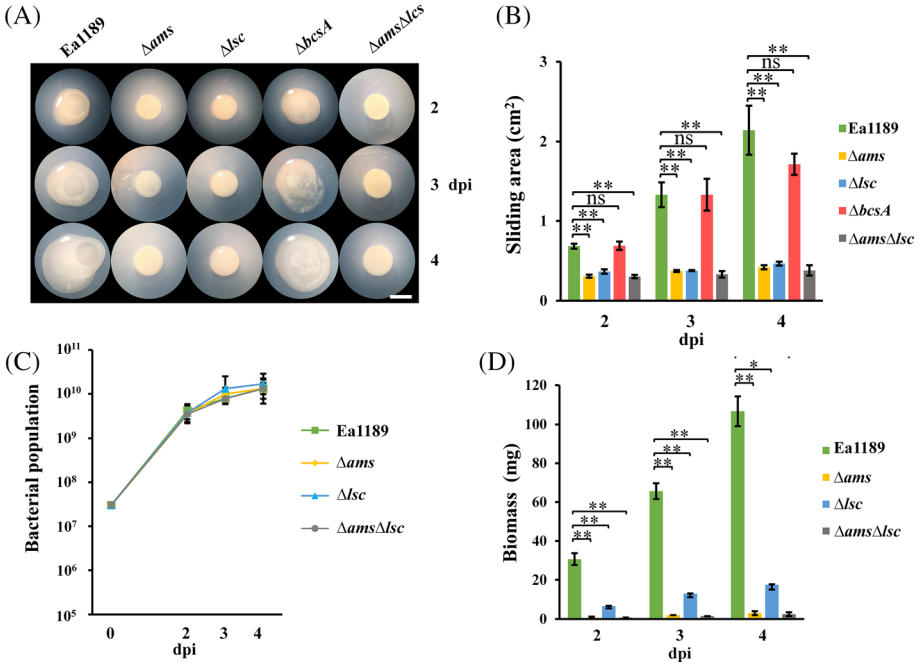

FIGURE 2 EPSs amylovoran and levan are required for sliding. (A) Microphotographs of bacterial sliding (A) and overall sliding areas (B) were determined in wild-type (WT) Ea1189 and several EPS-deficient mutant strains of Ea1189, including Ea1189Δ*ams*, Ea1189Δ*lsc*, Ea1189Δ*bcsA*, and Ea1189Δ*ams*Δ*lsc*, on 1.5% agar minimal medium (MM) at 2, 3, and 4 days post inoculation (dpi). The scale bar represents 0.5 cm. (C) Bacterial populations of WT Ea1189, Ea1189Δ*ams*, Ea1189Δ*lsc*, and Ea1189Δ*ams*Δ*lsc* were determined while cells were sliding on 1.5% agar MM at 0, 2, 3, and 4 dpi. (D) Weights of the total biomass produced by the sliding cells of Ea1189, Ea1189Δ*ams*, Ea1189Δ*lsc*, and Ea1189Δ*ams*Δ*lsc* were measured at 2, 3, and 4 dpi. Assays were performed as described in Experimental Procedures section. Mean and standard deviation ($n = 3$) are shown. One representative experiment was chosen, and three independent experiments were performed. Asterisks indicate statistically significant differences of the means (*$p < 0.05$, **$p < 0.01$ by Student's *t*-test). Ns, not significant

Sliding motility positively contributes to biomass without affecting bacterial population size

Bacteria migrate via various motility mechanisms to acquire nutrients (Ni et al., 2020; Yan et al., 2017). To investigate the role of sliding motility in *E. amylovora*, we measured the bacterial population and biomass of WT Ea1189 and various EPS-deficient mutants following cell sliding on 1.5% agar MM. Interestingly, no significant differences were observed in the number of cells between WT and EPS-deficient mutants at 2, 3, and 4 dpi (Figure 2C), implying that EPS-mediated sliding motility does not benefit *E. amylovora* for growth. This data also suggests that the impaired sliding motility of EPS-deficient mutants (Figure 2A,B) is not due to a growth defect.

We observed a consistent increase in the weight of biomass, consisting of extracellular materials and cells, of WT Ea1189 sliding on 1.5% agar MM (Figure 2D). Ea1189Δ*lsc*, whose amylovoran production was normal in a liquid environment (Figure S3), generated detectable biomass that was significantly reduced in weight relative to that of Ea1189 (Figure 2D). Moreover, the weight of biomass produced by two non-sliding amylovoran-deficient mutants, Ea1189Δ*ams* and Ea1189Δ*ams*Δ*lsc*, was barely detected (Figure 2D), which agrees with a previous study showing that MM broth-grown *E. amylovora* produces amylovoran as the main EPS (Yuan, McGhee, et al., 2021).

EPS-dependent osmotic pressure and water availability positively affect sliding motility

To understand how EPSs affect motility mechanisms, we sought to test the established model that osmotic pressure generated by EPS production drives sliding (Seminara et al., 2012; Yan et al., 2017). To this end, we compared the sliding motility of Ea1189 on MM containing 1%, 1.5%, and 2% agar, respectively. Given that lower agar concentrations generate higher osmotic pressure differences between EPS and agar plate and enhance water uptake (Yan et al., 2017), we validated the above hypothesis by showing that an increase in the sliding area of Ea1189 was detected corresponding to a reduced agar concentration (Figure 3A). Interestingly, we also found that Ea1189Δ*lsc* slid on 1% agar MM, whereas Ea1189Δ*ams* did not (Figure 3B), and

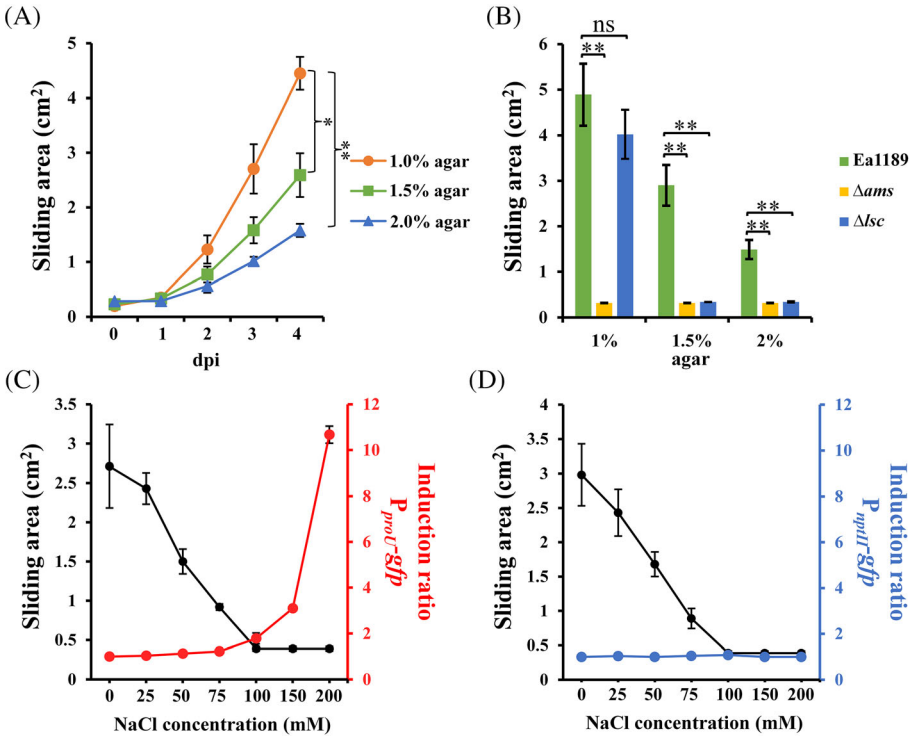

FIGURE 3 EPS-generated osmotic force drives sliding. (A) Sliding areas were determined on 1.0, 1.5, or 2.0% agar minimal medium (MM) for *E. amylovora* strain Ea1189 at 0, 1, 2, 3, and 4 days post inoculation (dpi) and (B) for Ea1189, Ea1189Δ*ams*, and Ea1189Δ*lsc* at 4 dpi. Sliding areas and induction of P_{proU}-*gfp* in Ea1189 harbouring the plasmid pPProGreen (C) or P_{nptII}-*gfp* in Ea1189 harbouring the plasmid pPNptGreen (D) were determined on 1.5% agar MM containing an increasing concentration of sodium chloride (NaCl) at 4 dpi, respectively. The induction ratio was calculated relative to the fluorescence of cells grown with 0 mM NaCl. Three independent experiments were performed in each experiment. Values are from one representative experiment. Error bars indicate standard deviations of the means ($n = 3$). Asterisks indicate statistically significant differences of the means ($p < 0.05$ by Student's *t*-test). Ns, not significant

neither of these mutants were motile on MM containing ≥1.5% agar (Figure 3B), indicating that both EPSs are needed for generating the maximum osmotic force.

Next, inspired by the importance of EPS-mediated osmotic pressure in sliding (Figure 3A) and the notion that EPSs are hydrated polymers mainly comprised of water (Sutherland, 1972), we hypothesized that water availability and water potential affect sliding. To address this question, we conducted sliding experiments on 1.5% agar MM supplemented with an increasing amount of sodium chloride (NaCl). Several studies demonstrated that NaCl is a permeating solute that reduces the water potential of the growth medium (Csonka, 1989; Halverson & Firestone, 2000). Indeed, the expression of a green fluorescence protein (GFP)-based transcriptional fusion P_{proU}-*gfp* that quantitatively responds to water deprivation (Axtell & Beattie, 2002) was induced by the addition of NaCl in a dose-dependent manner in Ea1189 (Figure 3C), confirming a lower water potential. More importantly, we found that the size of the sliding area was gradually decreased, and that no sliding phenotype was observed when 100 mM NaCl was added to the medium conferring a water potential of approximately −0.5 MPa (Figure 3C) (Axtell & Beattie, 2002). Bacterial populations were comparable between 0 and −0.5 MPa water potential on MM (Figure S5), which is consistent with a previous study showing that the population of *E. amylovora* was decreased only when the water potential was lower than −2 MPa in flower nectaries (Pusey, 2000). As a negative control, P_{nptII}-*gfp*, a water potential-independent reporter (Axtell & Beattie, 2002), expression was not altered in Ea1189 with or without the presence of NaCl (Figure 3D).

Lastly, surface wetting materials such as surfactants are known to facilitate bacterial movement (Harshey, 2003; Murray & Kazmierczak, 2008). In *E. amylovora*, we did not detect any surfactants produced (Figure S6), suggesting that a surfactant is likely not controlling or contributing to the sliding motility. Since one of the major functions of surfactants is to reduce the surface tension and increase the surface wettability (Shekhar et al., 2015), we measured the cell surface hydrophobicity of Ea1189, Ea1189Δ*ams*, and Ea1189Δ*lsc* and found that the cell surface of *E. amylovora* was highly hydrophilic with a value of hydrophobicity below 10%, and deletion of either *ams* or *lsc* did not significantly affect this value (Figure S7).

Impact of gravity and osmotic pressure on *E. amylovora* sliding

Gravity is a fundamental force; however, its impact on bacterial motility remains largely unknown (Acres et al., 2021). We observed a gravitational sliding motion for *E. amylovora*, as revealed when cells of Ea1189 were sliding on surfaces of 1.5% agar MM positioned at declined angles. From 10° to 20°, an increased slope assisted the downward sliding phenotype of Ea1189, and no sliding was observed for various EPS-deficient mutants (Figure 4A). Meanwhile, the osmotic pressure contrast created by EPS production and the availability of water were found to mediate sliding, a process for which flagella were not required (Figure 4B). We also observed that Ea1189 failed to climb on a 5° inclined surface of 1.5% agar MM (Figure 4A). Although *E. amylovora* formed a large bulk of slime consisting of EPSs (Figures 1, 2, and S1), our data indicate that the dynamic caused by EPS-generated osmotic force is unable to overcome gravity in directing the sliding motion of bacterial biomass on surfaces.

To further investigate how physical forces influence sliding, we assessed the movement of *E. amylovora* in confined environments, in which cells could migrate through a vertically placed 0.8-mm-wide microcapillary with walls comprised of 1.5% agar MM. Unlike unconfined environments where *E. amylovora* biomass did not propel upward (Figure 4A), we found that both Ea1189 and Ea1189Δ*flhDC1* exhibited upward sliding motility within the microcapillary (Figure 4C), and similar sliding lengths were observed for Ea1189 sliding up or down through the microcapillary (Figure 4C), indicating a negligible influence of gravity. On the other hand, EPS production is needed for bacterial sliding in a confined space, as Ea1189Δ*ams* was not motile within the microcapillary environment (Figure 4C).

Sliding motility is controlled by several EPS regulators and might act as a virulence factor

Bis-(3′-5′)-cyclic dimeric guanosine monophosphate (c-di-GMP) is a bacterial second messenger that positively regulates amylovoran production in *E. amylovora* (Edmunds et al., 2013; Kharadi et al., 2021). Deletion of genes *edcC* or *edcE*, encoding diguanylate cyclase enzymes necessary for c-di-GMP biosynthesis, resulted in reduced sliding motilities of Ea1189 on 1.5% agar MM (Figure 5A), suggesting that c-di-GMP positively contributes to sliding presumably via promoting amylovoran production. Complementation analysis by *in trans* expression of *edcC* or *edcE* restored the mutant phenotype to WT levels (Figure 5A). AmyR is a putative sensory transduction regulator protein and a major repressor of amylovoran (Zhao, Wang, et al., 2009). Interestingly, AmyR also upregulates the production of levan via an unknown mechanism (Wang et al., 2012). We found that the sliding areas produced by Ea1189Δ*amyR* were similar in size to those produced by Ea1189 at 2 and 3 dpi and were slightly reduced in size at 4 dpi (Figure 5B), and the expression of *amyR* from a plasmid (pBBR1-MCS5-*amyR*) strongly

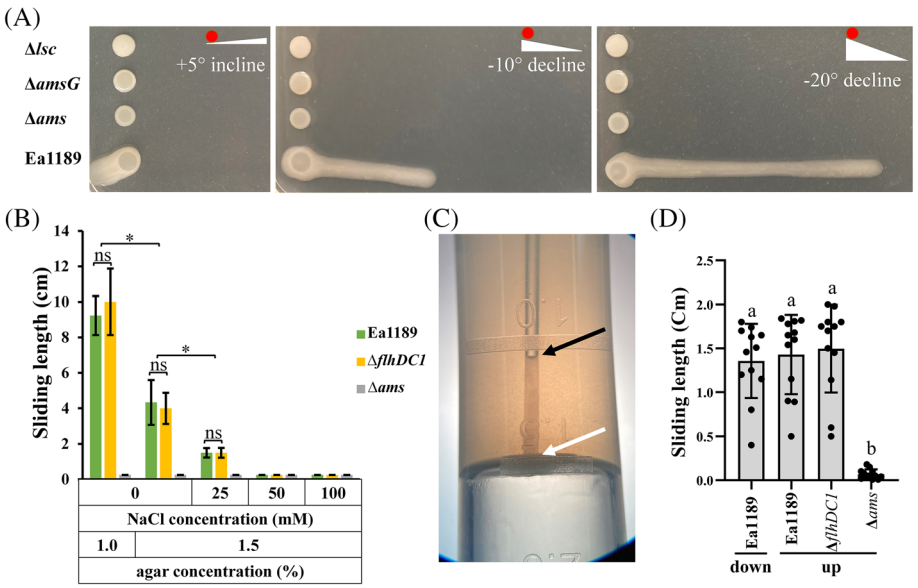

FIGURE 4 Gravity and EPS-based osmotic pressure affect sliding. (A) Sliding motility was determined on +5° inclined, −10° declined, or −20° declined 1.5% agar minimal medium (MM) surfaces for wild-type (WT) *E. amylovora* strain Ea1189, Ea1189Δ*ams*, Ea1189Δ*amsG*, and Ea1189Δ*lsc*, respectively. Filled red circles indicate the bacterial inoculation spot, following which the degree of inclined or declined surfaces is indicated by a filled white triangle. (B) Sliding lengths were measured on 10°-declined 1.0 or 1.5% agar MM for WT Ea1189, Ea1189Δ*flhDC1*, and Ea1189Δ*ams* with or without the presence of sodium chloride (NaCl). Mean and standard deviation ($n = 3$) are shown. (C) Arepresentative image showing *E. amylovora* slid up in a confined microcapillary. White and black arrows indicate the beginning and end of sliding over a 2-day period. Microphotograph was taken using light microscopy with transmitted lighting. (D) Sliding lengths were measured in vertically placed microcapillaries for WT Ea1189 (slid up or down) and Ea1189Δ*flhDC1* (slid up) and Ea1189Δ*ams* (slid up), respectively. Mean and standard deviation ($n = 12$) are shown. Assays were performed as described in experimental procedures. Three independent experiments were performed, and one representative experiment was chosen. Asterisks indicate statistically significant differences of the means ($p < 0.05$ by Student's *t*-test). Ns, not significant. Different lowercase letters above the bars indicate statistically significant differences between treatments (Fisher's least significant difference, $p < 0.05$).

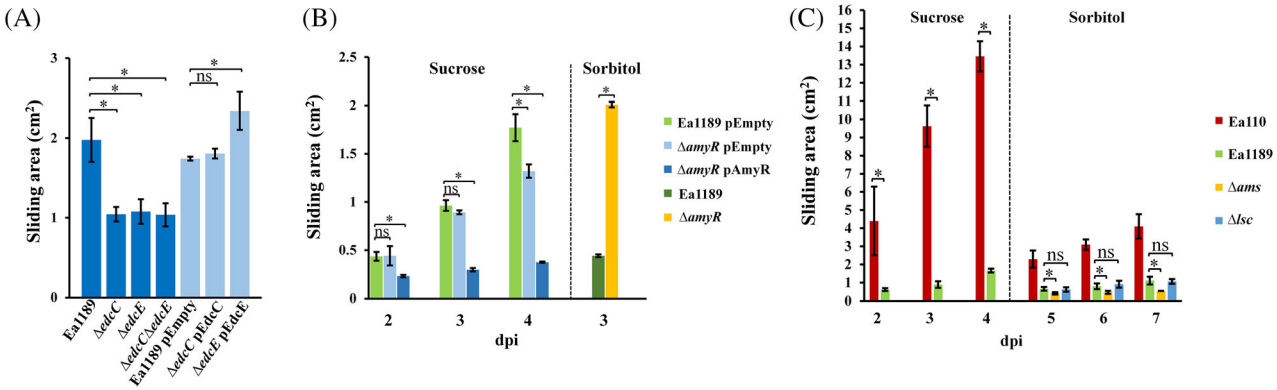

FIGURE 5 C-di-GMP, AmyR, and carbon sources affect sliding. (A) Sliding areas were measured on 1.5% agar minimal medium (MM) for wild-type (WT) *E. amylovora* strain Ea1189, mutant strains of Ea1189, including Ea1189Δ*edcC*, Ea1189Δ*edcE*, and Ea1189Δ*edcC*Δ*edcE*, Ea1189 harbouring the empty vector pBBR1-MCS5, Ea1189Δ*edcC* harbouring pBBR1-*edcC*, and Ea1189Δ*edcE* harbouring pBBR1-*edcE* at 4 days post inoculation (dpi). (B) Sliding motilities were compared between Ea1189 harbouring pBBR1-MCS5, Ea1189Δ*amyR* harbouring pBBR1-MCS5, and Ea1189Δ*amyR* harbouring pBBR1-*amyR* on 1.5% agar MM (MM-sucrose) at 2, 3, and 4 dpi, respectively. Sliding motilities were also compared between Ea1189 and Ea1189Δ*amyR* when cells were sliding on 1.5% agar MM-sorbitol at 3 dpi. (C) Overall sliding areas were measured for WT *E. amylovora* strain Ea110, WT Ea1189, Ea1189Δ*ams*, and Ea1189Δ*lsc* on 1.5% agar MM at 2, 3, and 4 dpi and on 1.5% agar MM-sorbitol at 5, 6, and 7 dpi, respectively. One representative experiment was chosen, and three independent experiments with three replicates were performed. Error bars indicate standard deviations of the means ($n = 3$). Asterisks indicate statistically significant differences of the means ($p < 0.05$ by Student's *t*-test). Ns, not significant

inhibited the sliding motility of Ea1189Δ*amyR* on 1.5% agar MM (Figure 5B). On 1.5% agar MM-sorbitol, a modified MM containing sorbitol, the primary storage carbohydrate in apples and other Rosaceae plants (Loescher, 1987), instead of sucrose to prevent the production of levan, our data showed that Ea1189Δ*amyR*

produced a sliding area that was 4-fold larger than that produced by Ea1189 at 3 dpi (Figure 5B). Taken together, these data are in line with our conclusion that both EPSs amylovoran and levan are required for the full sliding motility of *E. amylovora* on MM, as in a condition that only amylovoran but not levan is synthesized (MM-sorbitol), bacteria could still slide, but at a much slower pace. In addition, our observation agrees with a previous study showing that the rate of fire blight progression in apple shoots is negatively correlated with sorbitol concentration (Suleman & Steiner, 1994).

Different strains of *E. amylovora* have been reported to be genetically similar yet different in their levels of virulence (Cabrefiga & Montesinos, 2005; Puławska & Sobiczewski, 2012). A highly virulent *E. amylovora* strain Ea110 produces more amylovoran than the lower-virulent strain Ea1189, while the levansucrase activity was comparable (McGhee & Jones, 2000; Wang et al., 2010). We found that the enhanced amylovoran production indeed led to a significant increase in sliding areas for Ea110 relative to Ea1189 on either MM or MM-sorbitol (Figure 5C). As controls, Ea1189Δ*ams* failed to slide whereas Ea1189Δ*lsc* slid similar to Ea1189 on MM-sorbitol (Figure 5C). Collectively, we conclude that EPS-mediated sliding motility could act as a virulence factor of *E. amylovora*. When the sorbitol concentration is high, *E. amylovora* cells could migrate in host plants via producing amylovoran; however, when sucrose becomes the main carbon source, cells require the production of both amylovoran and levan for the maximum sliding motility.

Amylovoran and levan play different roles in sliding

To gain further insights into EPS-mediated sliding motility, we assessed the sliding behaviour of *E. amylovora* in co-inoculated mixtures of two strains (1:1 ratio), comprised of Ea1189 harbouring a plasmid constitutively expressing GFP and various EPS-deficient mutants harbouring a plasmid constitutively expressing mCherry. Microscopic images revealed that both Ea1189Δ*ams* and Ea1189Δ*lsc* slid in the presence of Ea1189 on 1.5% agar MM (Figure 6A,B), and we did not observe a rescued sliding motility in a mixture of Ea1189Δ*ams* and Ea1189Δ*lsc* (data not shown), highlighting an involvement of both EPSs in modulating the sliding motility of *E. amylovora*. Fluorescence proteins were not altering the sliding phenotype because similar sliding patterns were observed for Ea1189 and EPS-deficient mutants expressing either GFP or mCherry (Figures 1 and S8).

Interestingly, unlike Ea1189Δ*ams*, which slid similarly to Ea1189 in a mixture (Figure 6B), distinct differences were observed between Ea1189 and Ea1189Δ*lsc*, as cells of Ea1189Δ*lsc* were visualized mostly at the inoculated spot rather than at the margin of the sliding zone (Figure 6A). Quantitative analysis confirmed this observation showing that the number of cells of Ea1189Δ*lsc* was ~3.7 times more than that of Ea1189 around the inoculated spot and was ~3.2 times less in the sliding area (Figure S9). In contrast, cell numbers of Ea1189Δ*ams* were slightly less (~1.4 times) than Ea1189 only in the sliding area (Figure S9). These results collectively imply that extracellular complementation of levan from WT Ea1189 could not rescue the sliding motility of Ea1189Δ*lsc*, which is different from the amylovoran-mediated sliding motility.

We further validated this hypothesis by comparing the overall sliding area in conditions where WT Ea1189 cells were mixed with either live or dead cells of EPS-deficient mutants for sliding. As expected, no significant differences were observed between Ea1189 +- Ea1189Δ*lsc* and Ea1189 + Ea1189Δ*lsc*^{H} (^{H} represents cells were being heat treated at 95°C for 10 min) (Figure 6C), but the sliding area of Ea1189 +- Ea1189Δ*ams* was greatly reduced in size when compared with that of Ea1189 + Ea1189Δ*ams*^{H} (Figure 6C). Ea1189Δ*ams*Δ*lsc* was unable to produce either amylovoran or levan (Figure S3). Our data showed that cells of Ea1189Δ*ams*Δ*lsc* were less motile than Ea1189 during sliding similar to the single deletion mutant Ea1189Δ*lsc* (Figure 6A,D) and produced a much smaller sliding zone in Ea1189 + Ea1189Δ*ams*Δ*lsc* than that of Ea1189 + Ea1189Δ*ams*Δ*lsc*^{H} (Figure 6C), a phenotype the same as that of Ea1189Δ*ams* (Figure 6C). Taken together, these data indicate different roles of amylovoran and levan in controlling the sliding motility of *E. amylovora*. The association and possible physical linkage of levan with levan-producing cells are important for sliding, whereas the presence of exogenous amylovoran alone could power the sliding motility of amylovoran-deficient cells of *E. amylovora* (Figure 7).

DISCUSSION

In this work, we demonstrated that *E. amylovora* exhibits a unique surface motility mechanism driven by the production of two EPSs, amylovoran and levan. We further defined this as sliding motility, a mechanism initially described as a passive bacterial translocation powered by expansive forces created by cell division (Henrichsen, 1972; Hölscher & Kovács, 2017). It has been shown that *E. amylovora* produces mucoid colonies on minimal agar medium due to its ability to secrete EPS; in fact, early researchers used this growth morphology to distinguish *E. amylovora* from other *Erwinia* and *Pseudomonas* species and to rate its ability for EPS production in various naturally occurring strains (Falkenstein et al., 1988; Falkenstein et al., 1989). However, little is known regarding the

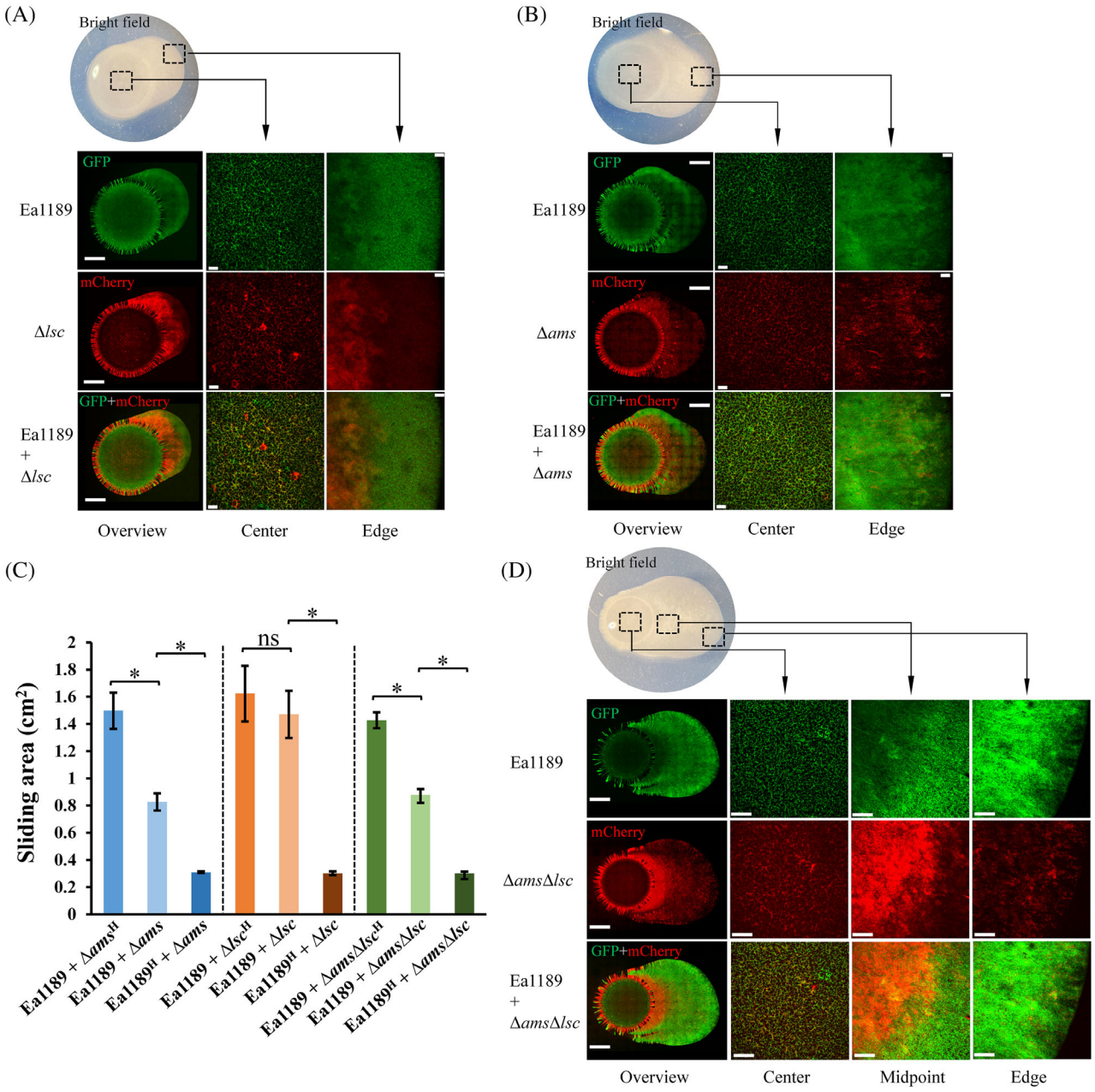

FIGURE 6 Sliding behaviours of *E. amylovora* in bacterial communities. Microphotographs were captured using light microscopy with incident lighting (bright field) and confocal laser scanning microscope detecting GFP (green) or mCherry (red). Ea1189 cells harbouring the plasmid pMP2444 were co-inoculated with Ea1189Δ*ams* (a) or Ea1189Δ*lsc* (B) harbouring the plasmid pBBR1-P_{nptII}-*mCherry* on 1.5% agar minimal medium at a ratio of 1:1. Cells were sliding for 4 days at 28°C. Microscopic overviews and closeups, showing cells from the inoculated spot (centre) and the edge of sliding (edge), were shown. (C) Overall sliding areas were measured in bacterial communities including Ea1189 + Ea1189Δ*ams*^{H}, Ea1189 + Ea1189Δ*ams*, Ea1189^{H} + Ea1189Δ*ams*, Ea1189 + Ea1189Δ*lsc*^{H}, Ea1189 + Ea1189Δ*lsc*, Ea1189^{H} + Ea1189Δ*lsc*, Ea1189 + Ea1189Δ*ams*Δ*lsc*^{H}, Ea1189 + Ea1189Δ*ams*Δ*lsc*, and Ea1189^{H} + Ea1189Δ*ams*Δ*lsc*^{H}. Represents cells were being heat-treated at 95°C for 10 min. Mean and standard deviation ($n = 3$) are shown. Asterisks indicate statistically significant differences of the means ($p < 0.05$ by Student's *t*-test). Ns, not significant. (D) Microphotographs showing sliding cells of Ea1189 harbouring pMP2444 and Ea1189Δ*ams*Δ*lsc* harbouring pBBR1-P_{nptII}-*mCherry*. Overviews and closeups, including centres, midpoints, and edges, were shown. Bars represent 0.2 cm in overviews, 0.1 mm in closeups of (a) and (B), and 0.2 mm in closeups of (D). Data are representative of three independent experiments.

consequence of EPS production on solid surfaces and, more importantly, how this affects the physiological behaviour of *E. amylovora* in vitro and *in planta*.

A unique feature of bacterial sliding is that this movement occurs independently of flagella (Hölscher & Kovács, 2017). The sliding motility phenotype reported in several bacterial systems, such as *P. aeruginosa* (Murray & Kazmierczak, 2008), *Salmonella enterica* serovar Typhimurium (Park et al., 2015), and *Serratia marcescens* (Matsuyama et al., 1992), is flagella-

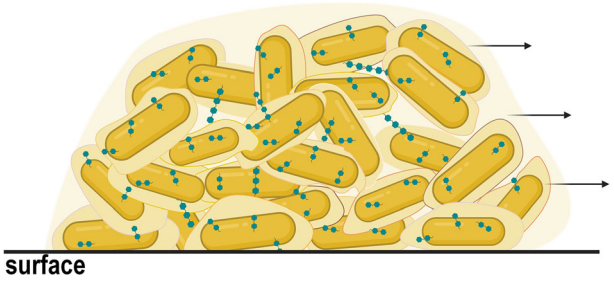

FIGURE 7 A graphical representation of EPS-mediated sliding motility in *E. amylovora*. *E. Amylovora* cells secrete levansucrase to catalyse the fructosyl transfer from sucrose to levan (blue hexagons) in the extracellular space. Levan is likely linked physically to the cell. Amylovoran is thought to be synthesized in the bacterial cytoplasm, polymerized in cell membranes, and secreted to the extracellular space. Amylovoran could attach to the cell as capsules (yellow circles around the bacterial cell) or secrete as a slime (a bigger yellow cloud around the biomass). Osmotic pressure gradients generated due to the EPS production could draw water from surrounding surfaces to the EPS matrix, resulting in sliding motility. Arrows indicate a sliding direction. The figure was created with BioRender.com.

independent in all cases. This is also true in *E. amylovora* as we found that the bacterial cells slide similarly in the presence or absence of flagella on surfaces of 1.5% agar plates or in confined microcapillaries (Figures 1 and 4). However, in soft agar (0.2%–0.4%), *E. amylovora* primarily uses flagella-based swimming and swarming for translocation (Figure 1A, B). These observations could be explained by the mechanics of flagella since flagellar filaments could rotate and generate torque more easily in liquid or semi-solid environments than on solid surfaces (Mandadapu et al., 2015), but it is more likely that *E. amylovora* has employed a complex signalling pathway, by which cells could switch between flagella-based and EPS-mediated motilities depending on different environmental conditions. Indeed, c-di-GMP, a key signalling component that represses swimming but induces biofilm formation in *E. amylovora* (Edmunds et al., 2013), was also involved in sliding (Figure 5A). c-di-GMP plays an important role in organismal sensing of environmental cues (Jenal et al., 2017; Sondermann et al., 2012). For example, several recent studies conducted in *Escherichia coli* and *P. aeruginosa* suggested that a higher surface stiffness could stimulate c-di-GMP signalling causing a reduction in flagella-based motility and enhanced biofilm development (Peng et al., 2019; Vrabioiu & Berg, 2022). Nevertheless, further studies are needed to fully understand the underlying mechanism that coordinates different motility mechanisms in *E. amylovora*.

Bacterial cells produce surfactants to reduce surface tension (Ron & Rosenberg, 2001), a process that has been reported to facilitate sliding behaviour (Hölscher & Kovács, 2017). For example, in *P. syringae* pv. *tomato* DC3000, Nogales and colleagues reported a surface sliding mechanism that relies heavily on the production of the biosurfactant syringafactin (Nogales et al., 2015). Our data indicated that *E. amylovora* does not produce surfactants (Figure S6), which is likely not a surprise because *E. amylovora* is best adapted to growth in the flower environment and in the interior of plants (apoplast and xylem), whereas *P. syringae* is particularly ubiquitous on leaves (Kharadi et al., 2021; Lindow & Brandl, 2003). Hydrophobins are also known to contribute to bacterial sliding. Grau et al. (2015) reported that BslA, a hydrophobin-like protein, acts as a water repellent for the sliding cells of *B. subtilis*. Since we found that the cell surface of *E. amylovora* was highly hydrophilic (Figure S7), whether and how hydrophobins affect *E. amylovora* sliding motility requires further investigation. We demonstrated here that the sliding motility of *E. amylovora* is mainly powered by the production of EPS in vitro similar to those characterized in *Sinorhizobium meliloti*, the soil-dwelling bacterium *B. subtilis*, and the plant pathogen *Xanthomonas citri* subsp. *citri* (Grau et al., 2015; Nogales et al., 2012; Seminara et al., 2012). Seminara and colleagues proposed osmotic pressure-driven sliding motility via the secretion of EPS in *B. subtilis* (Seminara et al., 2012), which has also been discovered in *V. cholerae* (Yan et al., 2017). Although specific evidence demonstrating that osmotic pressure physically spreads *E. amylovora* cells on surfaces is lacking, our data showed that water potential indeed positively contributes to sliding, and Yan et al. (2017) reported that an osmotic pressure differential could draw water into the secreted EPS matrix. Furthermore, T3SS and the type III effector DspA/E are pathogenicity factors of *E. amylovora* (Oh et al., 2005; Yuan, Hulin, & Sundin, 2021). A study conducted in *P. syringae* demonstrated that AvrE1, an *E. amylovora* DspA/E homologue, promotes stomatal closure and the occurrence of water-soaking lesions in host plants (Xin et al., 2016), and a similar phenotype has been reported in *X. gardneri* causing bacterial spot in tomato (Schwartz et al., 2017). The T3SS-mediated water-soaking lesions create an aqueous living space in the apoplast, which is essential for bacterial multiplication and disease development in the apoplast (Aung et al., 2018; El Kasmi et al., 2018; Gentzel et al., 2022; Roussin-Léveillée et al., 2022). A similar water-soaking lesion symptom caused by *E. amylovora* occurs during infection of apple flowers, infection of leaves at shoot tips, and in cankers (Van der Zwet and Keil, 1979). We hypothesize that the induction of an aqueous apoplast by *E. amylovora* facilitates the use of sliding motility to enable systemic spreading through host tissue without flagella.

Interestingly, unlike *V. cholerae* cells that acquire nutrients for growth by sliding (Yan et al., 2017), the sliding cells of *E. amylovora* showed comparable cell populations and enhanced production of biomass

consisting of EPS than those of the non-sliding mutants in vitro (Figure 2). These data signify the notion that EPS production is an energy-consuming process, but it remains to be determined how *E. amylovora* balances between virulence and fitness at the molecular level. Recently, we reported that a functional tricarboxylic acid (TCA) cycle is required for amylovoran production; when cells encounter low oxygen environments, *E. amylovora* could synthesize thiamine pyrophosphate, a cofactor of several TCA metabolic enzymes, to stimulate the TCA cycle thus providing energetic requirements to produce amylovoran (Yuan, McGhee, et al., 2021). In addition, unlike the in vitro medium environment where we conducted sliding experiments, the hydrated apoplast region of leaves accompanying water-soaking lesions would provide a ready source of water and nutrients that are leaking from plant host cells killed by the pathogen. This modified environment is likely conducive to both cell proliferation and increased EPS synthesis that furthers sliding motility and systemic spread through the plant (Figure 8). Furthermore, the high density of *E. amylovora* cells and EPS in parenchymal cell layers of the plant also contributes to the exudation of ooze droplets on the plant surface that function in pathogen dispersal (Slack et al., 2017; Thomson, 2000).

EPSs produced by *E. amylovora* have multiple functions ranging from modulating bacterial lifestyles to affecting the overall pathogenicity. Early studies demonstrated that amylovoran and levan are important structural components of biofilms formed by *E. amylovora* in vitro and *in planta* (Bellemann et al., 1994; Gross et al., 1992; Koczan et al., 2009). Castiblanco and Sundin (2018) showed that cellulose plays a role in shaping the biofilm matrix in vitro and contributes to the virulence of *E. amylovora* in an apple shoot model. More recently, amylovoran and cellulose have been reported to be involved in autoaggregation, a newly defined behaviour of *E. amylovora* in liquid environments (Kharadi & Sundin, 2019). Our data suggested that amylovoran and levan are required for sliding, which poses an intriguing question: why would *E. amylovora* use two different EPSs for its surface movement? This could be explained by the finding that amylovoran and levan exhibit different physiological functions for sliding, as we showed that, unlike amylovoran-deficient cells, mixing levan-deficient cells with WT bacteria did not rescue their sliding motility (Figure 6). Since amylovoran has been visualized as capsules attached to the bacterial cell wall that could also be released into the environment (Bellemann et al., 1994), we conclude that amylovoran plays a larger role in forming the bulk of the biomass for generating osmotic pressure (Figure 7). Water could then be drawn into the EPS matrix due to osmotic pressure differences, expanding the volume of biomass, and resulting in sliding motility (Figure 7). The localization of levan is poorly characterized. Our data indicate that levan, produced by levansucrase in the extracellular space, is likely associated with the cell membrane. Levan draws water from surrounding surfaces, and the resulting force together with the physical linkage between levan and cells could then push cells for sliding (Figure 7).

Lastly, how do *E. amylovora* cells migrate in the apoplast? This question has been a long-standing puzzle in the fire blight community. Despite flagella-dependent motilities being the only characterized translocation methods in *E. amylovora*, evidence from a large number of early studies and our data indicate that flagella are not required for the apoplastic migration of *E. amylovora* through infected trees (Bayot & Ries, 1986; Cesbron et al., 2006; Raymundo & Ries, 1981). Furthermore, a recent proteomic analysis showed that the presence of flagellar proteins might negatively affect the virulence of *E. amylovora* in the apoplast (Holtappels et al., 2018), possibly due to PAMP (pathogen-associated molecular pattern)-triggered plant immunity (Zhang & Zhou, 2010) caused by flagellar proteins such as flagellin. In this study, we discovered a passive surface translocation that is independent of flagella and flagella-based motilities in *E. amylovora*. In line with previous studies implying that EPS is likely the key player in powering the apoplastic migration of *E. amylovora* (Geider, 2000; Koczan et al., 2009; Slack et al., 2017), we showed that sliding is driven by two EPSs amylovoran and levan. This EPS-mediated motility was required for the in vitro translocation of bacteria in both unconfined and confined spaces and is likely to play a major role in the migration of *E. amylovora* cells *in planta*. In summary, we propose a model showing that the production of

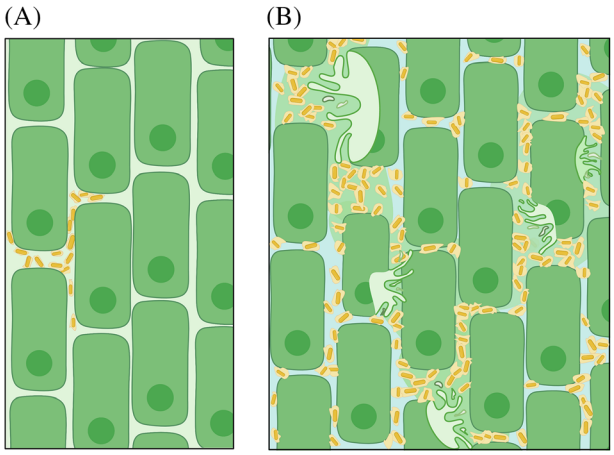

FIGURE 8 Model of the apoplast region of parenchymal cell layers of an apple leaf upon initiation of *E. amylovora* infection showing (A) a small number of invading cells establishing an infection, and (B) type three secretion mediated host cell death resulting in leakage of water and nutrients that result in hydration of the apoplast stimulating pathogen cell growth and increased EPS production that furthers sliding motility and systemic spread. The figure was created with BioRender.com.

EPSs by bacterial cells could draw the surrounding water to the polymers, thereby expanding the volume of biomass, and in the process, pushing the cell for sliding. Such a mechanism could be facilitated by the release of water and nutrients from plant cells caused by the T3SS-mediated cell death and are extremely efficient for spreading in confined spaces in the apoplast, as bacterial cells that are intimately bordered could expand simultaneously for sliding (Figure 8).

ACKNOWLEDGEMENTS

The authors thank Melinda K. Frame at the Centre for Advanced Microscopy at Michigan State University for the assistance with confocal microscopy, Janette L. Jacobs and Martin I. Chilvers for kindly providing the plasmid pmCherry_NAT, and Gwyn A. Beattie at Iowa State University for kindly providing the plasmids pPNptGreen and pPProGreen. The authors also thank Lindsay Brown for the assistance with figure creation. This project was supported by funds from the Agriculture and Food Research Initiative Competitive Grants Program Grants 2015-67013-23068 and 2020-51181-32158 from the USDA National Institute of Food and Agriculture and by Michigan State University AgBioResearch.

CONFLICT OF INTEREST

The author declares that there is no conflict of interest that could be perceived as prejudicing the impartiality of the research reported.

DATA AVAILABILITY STATEMENT

The data that support the findings of this study are available from the corresponding author upon reasonable request.

REFERENCES

Abràmoff, M.D., Magalhães, P.J. & Ram, S.J. (2004) Image processing with ImageJ. *Biophotonics International*, 11, 36–42.

Acres, J.M., Youngapelian, M.J. & Nadeau, J. (2021) The influence of spaceflight and simulated microgravity on bacterial motility and chemotaxis. *npj Microgravity*, 7, 1–11.

Aung, K., Jiang, Y. & He, S.Y. (2018) The role of water in plant–microbe interactions. *The Plant Journal*, 93, 771–780.

Axtell, C.A. & Beattie, G.A. (2002) Construction and characterization of a *proU*-gfp transcriptional fusion that measures water availability in a microbial habitat. *Applied and Environmental Microbiology*, 68, 4604–4612.

Bayot, R.G. & Ries, S.M. (1986) Role of motility in apple blossom infection by *Erwinia amylovora* and studies of fire blight control with attractant and repellent compounds. *Phytopathology*, 76, 441–445.

Beattie, G.A. (2011) Water relations in the interaction of foliar bacterial pathogens with plants. *Annual Review of Phytopathology*, 49, 533–555.

Bellemann, P., Bereswill, S., Berger, S. & Geider, K. (1994) Visualization of capsule formation by *Erwinia amylovora* and assays to determine amylovoran synthesis. *International Journal of Biological Macromolecules*, 16, 290–296.

Bellemann, P. & Geider, K. (1992) Localization of transposon insertions in pathogenicity mutants of *Erwinia amylovora* and their biochemical characterization. *Microbiology*, 138, 931–940.

Berg, H.C. (2003) The rotary motor of bacterial flagella. *Annual Review of Biochemistry*, 72, 19–54.

Blair, D.F. & Berg, H.C. (1990) The MotA protein of *E. coli* is a proton-conducting component of the flagellar motor. *Cell*, 60, 439–449.

Bugert, P. & Geider, K. (1995) Molecular analysis of the *ams* operon required for exopolysaccharide synthesis of *Erwinia amylovora*. *Molecular Microbiology*, 15, 917–933.

Burch, A.Y., Shimada, B.K., Browne, P.J. & Lindow, S.E. (2010) Novel high-throughput detection method to assess bacterial surfactant production. *Applied and Environmental Microbiology*, 76, 5363–5372.

Cabrefiga, J. & Montesinos, E. (2005) Analysis of aggressiveness of *Erwinia amylovora* using disease-dose and time relationships. *Phytopathology*, 95, 1430–1437.

Castiblanco, L.F. & Sundin, G.W. (2016) New insights on molecular regulation of biofilm formation in plant-associated bacteria. *Journal of Integrative Plant Biology*, 58, 362–372.

Castiblanco, L.F. & Sundin, G.W. (2018) Cellulose production, activated by cyclic di-GMP through BcsA and BcsZ, is a virulence factor and an essential determinant of the three-dimensional architectures of biofilms formed by *Erwinia amylovora* Ea1189. *Molecular Plant Pathology*, 19, 90–103.

Cesbron, S., Paulin, J.-P., Tharaud, M., Barny, M.-A. & Brisset, M.-N. (2006) The alternative σ factor HrpL negatively modulates the flagellar system in the phytopathogenic bacterium *Erwinia amylovora* under *hrp*-inducing conditions. *FEMS Microbiology Letters*, 257, 221–227.

Csonka, L.N. (1989) Physiological and genetic responses of bacteria to osmotic stress. *Microbiological Reviews*, 53, 121–147.

Datsenko, K.A. & Wanner, B.L. (2000) One-step inactivation of chromosomal genes in *Escherichia coli* K-12 using PCR products. *Proceedings of the National Academy of Sciences of the United States of America*, 97, 6640–6645.

Edmunds, A.C., Castiblanco, L.F., Sundin, G.W. & Waters, C.M. (2013) Cyclic Di-GMP modulates the disease progression of *Erwinia amylovora*. *Journal of Bacteriology*, 195, 2155–2165.

El Kasmi, F., Horvath, D. & Lahaye, T. (2018) Microbial effectors and the role of water and sugar in the infection battle ground. *Current Opinion in Plant Biology*, 44, 98–107.

Falkenstein, H., Bellemann, P., Walter, S., Zeller, W. & Geider, K. (1988) Identification of *Erwinia amylovora*, the fireblight pathogen, by colony hybridization with DNA from plasmid pEA29. *Applied and Environmental Microbiology*, 54, 2798–2802.

Falkenstein, H., Zeller, W. & Geider, K. (1989) The 29 kb plasmid, common in strains of *Erwinia amylovora*, modulates development of fireblight symptoms. *Microbiology*, 135, 2643–2650.

Fall, R., Kearns, D.B. & Nguyen, T. (2006) A defined medium to investigate sliding motility in a *Bacillus subtilis* flagella-less mutant. *BMC Microbiology*, 6, 1–11.

Fitzgerald, D.M., Bonocora, R.P. & Wade, J.T. (2014) Comprehensive mapping of the *Escherichia coli* flagellar regulatory network. *PLoS Genetics*, 10, e1004649.

Geider, K. (2000) Exopolysaccharides of *Erwinia amylovora*: structure, biosynthesis, regulation, role in pathogenicity of amylovoran and levan. In: Vanneste, J.L. (Ed.) *Fire blight: the disease its causative agent, Erwinia amylovora*. Wallingford, UK: CAB International, pp. 117–140.

Geier, G. & Geider, K. (1993) Characterization and influence on virulence of the levansucrase gene from the fireblight pathogen *Erwinia amylovora*. *Physiological and Molecular Plant Pathology*, 42, 387–404.

Gentzel, I., Giese, L., Ekanayake, G., Mikhail, K., Zhao, W., Cocuron, J.-C. et al. (2022) Dynamic nutrient acquisition from a hydrated apoplast supports biotrophic proliferation of a bacterial pathogen of maize. *Cell Host & Microbe*, 30, 502–517.e4.

Grau, R.R., de Oña, P., Kunert, M., Leñini, C., Gallegos-Monterrosa, R., Mhatre, E. et al. (2015) A duo of potassium-responsive histidine kinases govern the multicellular destiny of *Bacillus subtilis*. *mBio*, 6, e00581–e00515.

Griffith, C.S., Sutton, T.B. & Peterson, P.D. (2003) *Fire blight: the foundation of phytobacteriology*. St. Paul, MN, USA: APS press.

Gross, M., Geier, G., Rudolph, K. & Geider, K. (1992) Levan and levansucrase synthesized by the fireblight pathogen *Erwinia amylovora*. *Physiological and Molecular Plant Pathology*, 40, 371–381.

Halverson, L.J. & Firestone, M.K. (2000) Differential effects of permeating and nonpermeating solutes on the fatty acid composition of *Pseudomonas putida*. *Applied and Environmental Microbiology*, 66, 2414–2421.

Harshey, R.M. (2003) Bacterial motility on a surface: many ways to a common goal. *Annual Review of Microbiology*, 57, 249–273.

Henrichsen, J. (1972) Bacterial surface translocation: a survey and a classification. *Bacteriological Reviews*, 36, 478–503.

Hölscher, T. & Kovács, Á.T. (2017) Sliding on the surface: bacterial spreading without an active motor. *Environmental Microbiology*, 19, 2537–2545.

Holtappels, M., Noben, J.-P., Van Dijck, P. & Valcke, R. (2018) Fire blight host-pathogen interaction: proteome profiles of *Erwinia amylovora* infecting apple rootstocks. *Scientific Reports*, 8, 1–9.

Holtappels, M., Vrancken, K., Schoofs, H., Deckers, T., Remans, T., Noben, J.-P. et al. (2015) A comparative proteome analysis reveals flagellin, chemotaxis regulated proteins and amylovoran to be involved in virulence differences between *Erwinia amylovora* strains. *Journal of Proteomics*, 123, 54–69.

Jenal, U., Reinders, A. & Lori, C. (2017) Cyclic di-GMP: second messenger extraordinaire. *Nature Reviews. Microbiology*, 15, 271–284.

Kearns, D.B. (2010) A field guide to bacterial swarming motility. *Nature Reviews. Microbiology*, 8, 634–644.

Kharadi, R.R., Schachterle, J.K., Yuan, X., Castiblanco, L.F., Peng, J., Slack, S.M. et al. (2021) Genetic dissection of the *Erwinia amylovora* disease cycle. *Annual Review of Phytopathology*, 59, 191–212.

Kharadi, R.R. & Sundin, G.W. (2019) Physiological and microscopic characterization of cyclic-di-GMP-mediated autoaggregation in *Erwinia amylovora*. *Frontiers in Microbiology*, 10, 468.

Koczan, J.M., McGrath, M.J., Zhao, Y. & Sundin, G.W. (2009) Contribution of *Erwinia amylovora* exopolysaccharides amylovoran and Levan to biofilm formation: implications in pathogenicity. *Phytopathology*, 99, 1237–1244.

Kovach, M.E., Elzer, P.H., Hill, D.S., Robertson, G.T., Farris, M.A., Roop, R.M. et al. (1995) Four new derivatives of the broad-host-range cloning vector pBBR1MCS, carrying different antibiotic-resistance cassettes. *Gene*, 166, 175–176.

Leigh, J.A. & Coplin, D.L. (1992) Exopolysaccharides in plant-bacterial interactions. *Annual Review of Microbiology*, 46, 307–346.

Limoli, D.H., Jones, C.J. & Wozniak, D.J. (2015) Bacterial extracellular polysaccharides in biofilm formation and function. *Microbiol Spectrum*, 3, 29.

Lindow, S.E. & Brandl, M.T. (2003) Microbiology of the phyllosphere. *Applied and Environmental Microbiology*, 69, 1875–1883.

Loescher, W.H. (1987) Physiology and metabolism of sugar alcohols in higher plants. *Physiologia Plantarum*, 70, 553–557.

Malnoy, M., Martens, S., Norelli, J.L., Barny, M.-A., Sundin, G.W., Smits, T.H. et al. (2012) Fire blight: applied genomic insights of the pathogen and host. *Annual Review of Phytopathology*, 50, 475–494.

Mandadapu, K.K., Nirody, J.A., Berry, R.M. & Oster, G. (2015) Mechanics of torque generation in the bacterial flagellar motor. *Proceedings of the National Academy of Sciences of the United States of America*, 112, E4381–E4389.

Matsuyama, T., Kaneda, K., Nakagawa, Y., Isa, K., Hara-Hotta, H. & Yano, I. (1992) A novel extracellular cyclic lipopeptide which promotes flagellum-dependent and -independent spreading growth of *Serratia marcescens*. *Journal of Bacteriology*, 174, 1769–1776.

Mattick, J.S. (2002) Type IV pili and twitching motility. *Annual Review of Microbiology*, 56, 289–314.

McBride, M.J. (2001) Bacterial gliding motility: multiple mechanisms for cell movement over surfaces. *Annual Review of Microbiology*, 55, 49–75.

McGhee, G.C. & Jones, A.L. (2000) Complete nucleotide sequence of ubiquitous plasmid pEA29 from *Erwinia amylovora* strain Ea88: gene organization and intraspecies variation. *Applied and Environmental Microbiology*, 66, 4897–4907.

Minamino, T., Imada, K. & Namba, K. (2008) Molecular motors of the bacterial flagella. *Current Opinion in Structural Biology*, 18, 693–701.

Momol, M., Norelli, J., Piccioni, D., Momol, E., Gustafson, H., Cummins, J. et al. (1998) Internal movement of *Erwinia amylovora* through symptomless apple scion tissues into the rootstock. *Plant Disease*, 82, 646–650.

Murray, T.S. & Kazmierczak, B.I. (2008) *Pseudomonas aeruginosa* exhibits sliding motility in the absence of type IV pili and flagella. *Journal of Bacteriology*, 190, 2700–2708.

Ni, B., Colin, R., Link, H., Endres, R.G. & Sourjik, V. (2020) Growth-rate dependent resource investment in bacterial motile behavior quantitatively follows potential benefit of chemotaxis. *Proceedings of the National Academy of Sciences of the United States of America*, 117, 595–601.

Nimtz, M., Mort, A., Domke, T., Wray, V., Zhang, Y., Qiu, F. et al. (1996) Structure of amylovoran, the capsular exopolysaccharide from the fire blight pathogen *Erwinia amylovora*. *Carbohydrate Research*, 287, 59–76.

Nogales, J., Bernabéu-Roda, L., Cuéllar, V. & Soto, M.J. (2012) ExpR is not required for swarming but promotes sliding in *Sinorhizobium meliloti*. *Journal of Bacteriology*, 194, 2027–2035.

Nogales, J., Vargas, P., Farias, G.A., Olmedilla, A., Sanjuán, J. & Gallegos, M.-T. (2015) FleQ coordinates flagellum-dependent and-independent motilities in *Pseudomonas syringae* pv. Tomato DC3000. *Applied and Environmental Microbiology*, 81, 7533–7545.

Oh, C.-S., Kim, J.F. & Beer, S.V. (2005) The Hrp pathogenicity Island of *Erwinia amylovora* and identification of three novel genes required for systemic infection. *Molecular Plant Pathology*, 6, 125–138.

Park, S.-Y., Pontes, M.H. & Groisman, E.A. (2015) Flagella-independent surface motility in *Salmonella enterica* serovar Typhimurium. *Proceedings of the National Academy of Sciences of the United States of America*, 112, 1850–1855.

Peng, Q., Zhou, X., Wang, Z., Xie, Q., Ma, C., Zhang, G. et al. (2019) Three-dimensional bacterial motions near a surface investigated by digital holographic microscopy: effect of surface stiffness. *Langmuir*, 35, 12257–12263.

Puławska, J., Kałużna, M., Warabieda, W. & Mikiciński, A. (2017) Comparative transcriptome analysis of a lowly virulent strain of *Erwinia amylovora* in shoots of two apple cultivars-susceptible and resistant to fire blight. *BMC Genomics*, 18, 868.

Puławska, J. & Sobiczewski, P. (2012) Phenotypic and genetic diversity of *Erwinia amylovora*: the causal agent of fire blight. *Trees*, 26, 3–12.

Pusey, P. (2000) The role of water in epiphytic colonization and infection of pomaceous flowers by *Erwinia amylovora*. *Phytopathology*, 90, 1352–1357.

Raymundo, A. & Ries, S. (1981) Motility of *Erwinia amylovora*. *Phytopathology*, 70, 1062–1065.

Recht, J. & Kolter, R. (2001) Glycopeptidolipid acetylation affects sliding motility and biofilm formation in *Mycobacterium smegmatis*. *Journal of Bacteriology*, 183, 5718–5724.

Ritchie, D. & Klos, E. (1977) Isolation of *Erwinia amylovora* bacteriophage from aerial parts of apple trees. *Phytopathology*, 67, 101–104.

Ron, E.Z. & Rosenberg, E. (2001) Natural roles of biosurfactants: minireview. *Environmental Microbiology*, 3, 229–236.

Ross, P., Mayer, R. & Benziman, M. (1991) Cellulose biosynthesis and function in bacteria. *Microbiological Reviews*, 55, 35–58.

Roth, M.G. & Chilvers, M.I. (2019) A protoplast generation and transformation method for soybean sudden death syndrome causal

agents *Fusarium virguliforme* and *F. brasiliense*. *Fungal BiologyBiotechnology*, 6, 1–8.
Roussin-Léveillée, C., Lajeunesse, G., St-Amand, M., Veerapen, V. P., Silva-Martins, G., Nomura, K. et al. (2022) Evolutionarily conserved bacterial effectors hijack abscisic acid signaling to induce an aqueous environment in the apoplast. *Cell Host & Microbe*, 30, 489–501.e4.
Schachterle, J.K., Zeng, Q. & Sundin, G.W. (2019) Three Hfq-dependent small RNAs regulate flagellar motility in the fire blight pathogen *Erwinia amylovora*. *Molecular Microbiology*, 111, 1476–1492.
Schwartz, A.R., Morbitzer, R., Lahaye, T. & Staskawicz, B. (2017) TALE-induced bHLH transcription factors that activate a pectate lyase contribute to water soaking in bacterial spot of tomato. *Proceedings of the National Academy of Sciences of the United States of America*, 114, E897–E903.
Seemüller, E. & Beer, S. (1977) Isolation and partial characterization of two neutral proteases of *Erwinia amylovora*. *Journal of Phytopathology*, 90, 12–21.
Seminara, A., Angelini, T.E., Wilking, J.N., Vlamakis, H., Ebrahim, S., Kolter, R. et al. (2012) Osmotic spreading of *Bacillus subtilis* biofilms driven by an extracellular matrix. *Proceedings of the National Academy of Sciences of the United States of America*, 109, 1116–1121.
Shekhar, S., Sundaramanickam, A. & Balasubramanian, T. (2015) Biosurfactant producing microbes and their potential applications: a review. *Critical Reviews in Environmental Science and Technology*, 45, 1522–1554.
Slack, S.M., Zeng, Q., Outwater, C.A. & Sundin, G.W. (2017) Microbiological examination of Erwinia amylovora exopolysaccharide ooze. *Phytopathology*, 107, 403–411.
Sondermann, H., Shikuma, N.J. & Yildiz, F.H. (2012) You've come a long way: c-di-GMP signaling. *Current Opinion in Microbiology*, 15, 140–146.
Stuurman, N., Bras, C.P., Schlaman, H.R., Wijfjes, A.H., Bloemberg, G. & Spaink, H.P. (2000) Use of green fluorescent protein color variants expressed on stable broad-host-range vectors to visualize rhizobia interacting with plants. *Molecular Plant-Microbe Interactions*, 13, 1163–1169.
Suleman, P. & Steiner, P.W. (1994) Relationship between sorbitol and solute potential in apple shoots relative to fire blight symptom development after infection by *Erwinia amylovora*. *Phytopathology*, 84, 1244.
Sutherland, I. (1972) Bacterial exopolysaccharides. *Advances in Microbial Physiology*, 8, 143–213.
Sutherland, I. (1982) Biosynthesis of microbial exopolysaccharides. *Advances in Microbial Physiology*, 23, 79–150.
Sutherland, I.W. (2001) Biofilm exopolysaccharides: a strong and sticky framework. *Microbiology*, 147, 3–9.
Thomson, S. (1986) The role of the stigma in fire blight infections. *Phytopathology*, 76, 476–482.
Thomson, S.V. (2000) Epidemiology of fire blight. In: *Fire blight: the disease and its causative agent, Erwinia amylovora*. Wallingfort UK: *CABI Publishing*, pp. 9–37.
Van Der Zwet, T. & H.L. Keil. (1979) Fire blight: A bacterial disease of rosaceous plants. No. 510. *US Department of Agriculture*.
Van Gestel, J., Vlamakis, H. & Kolter, R. (2015) From cell differentiation to cell collectives: *Bacillus subtilis* uses division of labor to migrate. *PLoS Biology*, 13, e1002141.
van Loosdrecht, M., Lyklema, J., Norde, W., Schraa, G. & Zehnder, A. (1987) The role of bacterial cell wall hydrophobicity in adhesion. *Applied and Environmental Microbiology*, 53, 1893–1897.
Vrabioiu, A.M. & Berg, H.C. (2022) Signaling events that occur when cells of *Escherichia coli* encounter a glass surface. *Proceedings of the National Academy of Sciences of the United States of America*, 119, e2116830119.
Wang, D., Korban, S.S., Pusey, P.L. & Zhao, Y. (2012) AmyR is a novel negative regulator of amylovoran production in *Erwinia amylovora*. *PLoS One*, 7, e45038.
Wang, D., Korban, S.S. & Zhao, Y. (2010) Molecular signature of differential virulence in natural isolates of *Erwinia amylovora*. *Phytopathology*, 100, 192–198.
Wang, S., Fleming, R.T., Westbrook, E.M., Matsumura, P. & McKay, D.B. (2006) Structure of the *Escherichia coli* FlhDC complex, a prokaryotic heteromeric regulator of transcription. *Journal of Molecular Biology*, 355, 798–808.
Whitfield, C., Wear, S.S. & Sande, C. (2020) Assembly of bacterial capsular polysaccharides and exopolysaccharides. *Annual Review of Microbiology*, 74, 521–543.
Xin, X.-F., Nomura, K., Aung, K., Velásquez, A.C., Yao, J., Boutrot, F. et al. (2016) Bacteria establish an aqueous living space in plants crucial for virulence. *Nature*, 539, 524–529.
Yan, J., Nadell, C.D., Stone, H.A., Wingreen, N.S. & Bassler, B.L. (2017) Extracellular-matrix-mediated osmotic pressure drives *vibrio cholerae* biofilm expansion and cheater exclusion. *Nature Communications*, 8, 1–11.
Yu, M., Singh, J., Khan, A., Sundin, G.W. & Zhao, Y.F. (2020) Complete genome sequence of the fire blight pathogen *Erwinia amylovora* strain Ea1189. *Molecular Plant-Microbe Interactions*, 33, 1277–1279.
Yuan, X., Eldred, L.I., Kharadi, R.R., Slack, S.M. & Sundin, G.W. (2022) The RNA-binding protein ProQ impacts exopolysaccharide biosynthesis and second messenger cyclic di-GMP signaling in the fire blight pathogen *Erwinia amylovora*. *Applied and Environmental Microbiology*, 88, e0023922.
Yuan, X., Hulin, M.T. & Sundin, G.W. (2021) Effectors, chaperones, and harpins of the Type III secretion system in the fire blight pathogen *Erwinia amylovora*: a review. *Journal of Plant Pathology*, 103, S25–S39.
Yuan, X., McGhee, G., Slack, S. & Sundin, G.W. (2021) A novel signaling pathway that connects thiamine biosynthesis, bacterial respiration, and production of the exopolysaccharide amylovoran in *Erwinia amylovora*. *Molecular Plant-Microbe Interactions*, 34, 1193–1208.
Zhang, J. & Zhou, J.-M. (2010) Plant immunity triggered by microbial molecular signatures. *Molecular Plant*, 3, 783–793.
Zhao, Y., Qi, M. & Wang, D. (2011) Evolution and function of flagellar and non-flagellar type III secretion systems in *Erwinia amylovora*. *Acta Horticulturae*, 896, 177–184.
Zhao, Y., Sundin, G.W. & Wang, D. (2009) Construction and analysis of pathogenicity Island deletion mutants of *Erwinia amylovora*. *Canadian Journal of Microbiology*, 55, 457–464.
Zhao, Y., Wang, D., Nakka, S., Sundin, G.W. & Korban, S.S. (2009) Systems level analysis of two-component signal transduction systems in *Erwinia amylovora*: role in virulence, regulation of amylovoran biosynthesis and swarming motility. *BMC Genomics*, 10:245, 1–16.
Zhong, M., Cywiak, C., Metto, A.C., Liu, X., Qian, C. & Pelled, G. (2021) Multi-session delivery of synchronous rTMS and sensory stimulation induces long-term plasticity. *Brain Stimulation*, 14, 884–894.

SUPPORTING INFORMATION

Additional supporting information can be found online in the Supporting Information section at the end of this article.

How to cite this article: Yuan, X., Eldred, L.I. & Sundin, G.W. (2022) Exopolysaccharides amylovoran and levan contribute to sliding motility in the fire blight pathogen *Erwinia amylovora*. *Environmental Microbiology*, 24(10), 4738–4754. Available from: https://doi.org/10.1111/1462-2920.16193